Cedar Lake, Wisconsin - Limnological response to alum treatment: 2018 interim report

1 December, 2018

University of Wisconsin – Stout
Sustainability Sciences Institute - Center for
Limnological Research and Rehabilitation
Department of Biology
123E Jarvis Hall
Menomonie, Wisconsin 54751
715-338-4395
jamesw@uwstout.edu

Harmony Environmental
516 Keller Ave S
Amery, Wisconsin 54001
715-268-9992
harmonyenv@amerytel.net

Executive Summary

- Post-Al treatment mean summer (Jul-Aug) concentrations of surface total phosphorus (P) and chlorophyll were lower in 2018 compared to pretreatment conditions. In particular, mean summer chlorophyll was only 19 μg/L in 2018, representing a 60% improvement over the 2010 summer mean of 48 μg/L.
- Bottom total P and soluble reactive P (SRP) concentrations were low until late July 2018. Concentrations increased to ~ 0.47 mg/L in August, suggesting Al binding efficiency for internal P loads had decreased. Nevertheless, net internal P loading in 2018, determined by P mass balance, was reduced by ~ 70% relative to 2010 (1,062 kg v 3,723 kg, respectively).
- An alum treatment, with dosages ranging between ~20 g/m^2 over depths between 20-25 ft and 26 g/m^2 over depths greater than 25 ft, is recommended for late June 2019 to continue suppression of internal P loading in Cedar Lake.

Objective

Multiple Al applications over a period of 12 years are planned for Cedar Lake in order to control internal phosphorus loading. It is critical to conduct post-treatment monitoring of water and sediment chemistry to document the trajectory of water quality improvement during rehabilitation to make informed decisions regarding adjusting management to meet future water quality goals. Post-treatment monitoring included field and laboratory research to document changes in 1) hydrology and watershed phosphorus (P) loading, 2) the P budget and lake water quality, 3) binding of sediment mobile P fractions that have contributed to internal P loading by alum, and 4) rates of diffusive P flux from the sediment under anaerobic conditions. Overall, lake water quality is predicted to respond to watershed and internal P loading reduction with lower surface concentrations of total P and chlorophyll concentrations throughout the summer, lower bloom frequency of nuisance chlorophyll levels, and higher water transparency. Multiple Al applications between 2017 and 2029 should result in the binding of iron-bound P and substantial reduction in diffusive P flux from sediments under anaerobic conditions (i.e., internal P loading). The objectives of this interim report were to describe the 2018 limnological and sediment variable response to the 2017 alum treatment in Cedar Lake.

Methods

Watershed loading and lake monitoring

A gauging station was established on Horse Creek above Cedar Lake at 10th Ave for concentration, loading, and flow determination between May and October 2018 (Fig. 1). Grab samples were collected biweekly at the 10th Ave gauging station for chemical analysis. Water samples were analyzed for TSS, total P, and soluble reactive P (SRP) using standard methods (APHA 2011, Wisconsin State Lab of Hygiene). Summer tributary P loading was calculated using the computer program FLUX.

The deep basin water quality station WQ 2 was sampled biweekly between May and October 2018 (Fig. 1). An integrated sample over the upper 2-m was collected for analysis of total P, SRP, and chlorophyll a. An additional discrete sample was collected within 0.5 m of the sediment surface for analysis of total and SRP. Secchi transparency and in situ measurements (temperature, dissolved oxygen, pH, and conductivity) were collected on each date using a YSI 6600 sonde (Yellow Springs Instruments) that was calibrated against dissolved oxygen Winkler titrations (APHA 2011) and known buffer solutions.

Sediment chemistry

Sediment characteristics. A sediment core was collected in July 2018 at WQ 2 for determination of vertical profiles of various sediment characteristics and phosphorus fractions (see Analytical methods below). The sediment core was sectioned at 1-cm intervals between 0 and 10 cm and at 2-cm intervals below the 10-cm depth for determination of moisture content, wet and dry bulk density, loss-on-ignition organic matter, loosely-bound P, iron-bound P, labile organic P, and aluminum-bound P.

Laboratory-derived diffusive phosphorus flux from sediments under anaerobic conditions. Anaerobic diffusive P fluxes were measured from intact sediment cores collected at stations

shown in Figure 1 in July 2018. One sediment core was collected at each station to monitor alum treatment effectiveness after application. The sediment incubation systems were placed in a darkened environmental chamber and incubated at 20 C for up to 5 days. The incubation temperature was set to a standard temperature for all stations for comparative purposes. The oxidation-reduction environment in each system was controlled by gently bubbling nitrogen through an air stone placed just above the sediment surface to maintain anaerobic conditions.

Water samples for SRP were collected from the center of each system using an acid-washed syringe and filtered through a 0.45 µm membrane syringe filter (Nalge). The water volume removed from each system during sampling was replaced by addition of filtered lake water preadjusted to the proper oxidation-reduction condition. These volumes were accurately measured for determination of dilution effects. Rates of P release from the sediment (mg/m^2 d) were calculated as the linear change in mass in the overlying water divided by time (days) and the area (m^2) of the incubation core liner. Regression analysis was used to estimate rates over the linear portion of the data.

Analytical methods. A known volume of sediment was dried at 105 ^oC for determination of moisture content, wet and dry bulk density, and burned at 550 ^oC for determination of loss-on-ignition organic matter content (Avnimelech et al. 2001, Håkanson and Jansson 2002). Phosphorus fractionation was conducted according to Hieltjes and Lijklema (1980), Psenner and Puckso (1988), and Nürnberg (1988) for the determination of ammonium-chloride-extractable P (loosely-bound P), bicarbonate-dithionite-extractable P (i.e., iron-bound P), and sodium hydroxide-extractable P (i.e., aluminum-bound P).

The loosely-bound and iron-bound P fractions are readily mobilized at the sediment-water interface as a result of anaerobic conditions that lead to desorption of P from sediment and diffusion into the overlying water column (Mortimer 1971, Boström et al. 1982, Boström 1984, Nürnberg 1988). The sum of the loosely-bound and iron-bound P fraction represents redox-sensitive P (i.e., the P fraction that is active in P release under anaerobic and reducing conditions) and will be referred to as ***redox-P***. Aluminum-bound P reflects P bound to the Al floc after aluminum sulfate application and its chemical transformation to aluminum hydroxide

($Al(OH)_3$).

Summary of Results

Hydrology and phosphorus loading

On an annual basis, precipitation in 2018 was slightly higher at ~39 inches compared to the ~ 33-inch average since 1980 (Fig. 2). Monthly precipitation exceeded the long-term average in July, September, and October 2018 (Fig. 3). Monthly precipitation was much less than the long-term average in June 2018.

Horse Creek summer flow exhibited minor peaks between May and June 2018 but was otherwise nominal in conjunction with below average precipitation during that period (Fig. 4). In particular, flow peaks were very minor in June and early July even though daily precipitation approached 2 inches on two occasions. This pattern suggested potential infiltration versus runoff. Major peaks in flow occurred in mid-August that coincided with a series of precipitation events. The highest measured flow event occurred in mid-September as a result of a nearly 3-inch precipitation event. Horse Creek mean summer (May-October) daily flow was 0.38 m^3/s, which fell slightly below ranges measured between 2009-2011 (James 2014; 2009 = 0.44 m^3/s, 2010 = 0.50 m^3/s, 2011 = 0.67 m^3/s).

Total P concentrations were elevated in May and June 2018 despite minor peaks in flow as a result of precipitation and runoff (Fig. 5). Reasons for this pattern are not precisely known but suggest the occurrence of some particulate P input that may not have been associated with runoff. In contrast, SRP was relatively low during this late spring period but then increased to ~ 0.06 mg/L in late June through early July in association with precipitation-related small peaks in the hydrograph. Concentrations of both constituents declined during the lower flow period of late July-early August, then increased to peaks in mid-September in conjunction with frequent rains in late summer.

Concentration-flow relationships in 2018 deviated slightly from those in 2009-2011 and 2017 primarily because P concentrations were relatively high in May and early June 2018 under lower flow conditions (Fig. 6). Flow-averaged summer (May through October) total P and SRP in 2018 were 0.100 mg/L and 0.039 mg/L, respectively, slightly higher than averages estimated for 2017 (Table 1). The flow-averaged SRP concentration accounted for ~ 40% of the total P in 2018. Summer total P and SRP loadings from Horse Creek were 3.36 and 1.28 kg/d (Table 1), respectively, in 2018, similar to previous research in 2009-11 and 2017.

Table 1. Mean summer constituent concentrations and loading for the Horse Creek inflow station at 10th Ave.

Year	Variable	TSS	Total P	SRP
2010	Concentration (mg/L)		0.089	0.031
	Load (kg/d)		4.18	1.42
2017	Concentration (mg/L)	15.2	0.084	0.034
	Load (kg/d)	767.8	4.26	1.71
2018	Concentration (mg/L)	16.5	0.100	0.039
	Load (kg/d)	549	3.36	1.28

Lake limnological response

Cedar Lake was stratified between late-May and early-September 2018 (Fig. 7). Complete water column mixing and turnover occurred in mid-September 2018. Bottom water anoxia was established between mid-May and early-September 2018. Anoxia extended only to about 6.5 m in 2018 compared to ~ 5.5 m in 2010. This pattern may have been related to reduced algal productivity, resulting in less organic carbon deposition to fuel sediment dissolved oxygen demand.

Similar to 2017 (i.e., alum treatment year), total P and SRP concentrations remained very low in the bottom waters (i.e., ~ 7.5 m depth) between the onset of hypolimnetic anoxia in May and the end of July 2018 (Fig. 8). Unlike patterns in 2017, concentrations of both P fractions increased in early August and exhibited peak concentrations of ~ 0.56 mg/L and 0.47 mg/L, respectively, in early September, suggesting that sediment diffusive P flux (i.e., internal P loading) was beginning to overwhelm Al floc binding efficiency. However, concentration peaks were much lower in 2018 compared to those in 2010 (i.e., > 1.0 mg/L P) and high concentrations of hypolimnetic P were confined to ~ 0.5 m above the sediment-water interface (Fig. 9).

Surface total P was relatively low between May and mid-August 2018, gradually increasing in

concentration over this time period (Fig. 8). A similar pattern of surface total P concentration increase occurred after the 2017 Al treatment. Unlike 2017 patterns, total P increased substantially in late September 2018. However, this increase was not associated with an algal bloom and increase in chlorophyll, as discussed further below, suggesting P was not incorporated into algal biomass (Fig. 10). Instead, peak surface total P coincided with high precipitation, elevated Horse Creek flow, and high concentrations of total P and SRP in the inflow (Fig. 5). Elevated total P and SRP concentrations were also observed throughout the upper 4-m water column during the late September high inflow event, further suggesting influences from the late September storm inflows (Fig. 9).

Surface chlorophyll concentrations were relatively low throughout the summer and fall of 2018 (Fig. 10). The concentration was very low between June and late July, 2018, ranging between only ~ 6 μg/L and ~ 14 μg/L. Unlike patterns in 2017, chlorophyll increased September-October 2018, but only to ~24-29 μg/L. Even though late fall storms resulted in apparently high lake SRP concentrations, chlorophyll remained low in concentration in October. With the exception of 2 dates in late September-early October that were influenced by the 2-inch rain event, there was a strong linear relationship between total P and chlorophyll, suggesting P-limitation of algal growth (Fig. 12). Storms in late September coincided with anonymously higher total P compared to chlorophyll, indicating that a significant portion of this P was not incorporated into algal biomass and may have been associated with detritus or eroded soil from the watershed.

By comparison, chlorophyll increased to ~ 40 μg/L in early September, 2017 (Fig. 10). However, this fall 2017 bloom was dominated by *Ceratium hirundinella* (not cyanobacteria), which otherwise occurred infrequently and was a rare part of the species assemblage in 2009-2011. Since *C. hirundinella* forms dormant resting cysts that reside in the sediment, it may have had a competitive advantage and exploited an otherwise empty niche after the 2017 alum treatment. While other algal species became severely P-limited after the alum treatment, *C. hirundinella* cysts may have stored surplus cellular P prior to the treatment that was used for growth during inoculation of the water column.

The typical seasonal chlorophyll pattern in years prior to alum treatment was a substantial

increase concentration during Fall turnover due to entrainment of hypolimnetic SRP and uptake by cyanobacteria (James et al. 2015). For instance, in 2010 chlorophyll increased from ~ 22 µg/L in mid-July to a maximum ~ 110 µg/L in early October (Fig. 10). Unlike Fall patterns in 2017 and 2018, chlorophyll concentrations remained high and maximal for extended periods (i.e., September through early November) during Fall turnover as in 2010. Thus, reduced hypolimnetic SRP availability as a result of alum treatment in 2017 led to much lower chlorophyll concentrations during the Fall turnover periods of 2017 and 2018.

Secchi transparency remained improved in conjunction with alum treatment in 2017 (Fig. 11). Prior to alum treatment, as in 2010, Secchi transparency was often unusually high in June, exceeding 2 to 3 m (James 2014, 2015). Transparency declined to a minimum (< 1.0 m) during periods of extended cyanobacteria blooms driven by Fall turnover and hypolimnetic SRP entrainment (Fig. 11, 2010). In 2018, Secchi transparency was highest between May and late July. Although it declined in August through September, transparency exceeded 1.0 to 1.5 m. Secchi transparency exhibited a significant inverse pattern to that of chlorophyll, indicating that light extinction was due to algae versus inorganic turbidity (Fig. 12). Thus, lower chlorophyll concentrations translated into higher Secchi transparency, particularly during the Fall of 2017 and 2018.

A comparison of mean summer (July-early October) limnological response variables before alum treatment (i.e., 2010) versus 2018 is shown in Figure 13 and Table 2. Mean bottom total P and SRP increased in 2018 compared to 2017 but concentrations were still low relative to the pretreatment year 2010. Mean bottom total P and SRP concentrations in 2018 were ~ 57% lower compared to pretreatment 2010 means (Table 2). Mean summer surface total P increased slightly in 2018, which may have been more related to late September P loading from the watershed versus algal biomass. Nevertheless, the mean was 22% lower compared to 2010 (Table 2). Mean chlorophyll was actually lower in 2018 versus 2017, which was likely attributed to the occurrence of a rare *C. hirundinella* bloom that occurred in 2017. The 2018 chlorophyll mean represented a 60% improvement over the pretreatment 2010 mean (Table 2). Finally, mean Secchi transparency declined by ~ 1.2 ft in 2018 versus 2017. But, this pattern may have been

Table 2. Summary of changes in lake water quality and sediment variables after the initial alum treatment in June 2017. Overall goals after completion of the treatment schedule are shown in the last column.

Variable			2010	2017	2018	Percent improvement over 2010 means		Goal after internal P loading control
						2017	2018	
Lake	Mean (Jul-Oct)	Mean surface TP (mg/L)	0.074	0.051	0.058	31% reduction	22% reduction	< 0.035
		Mean bottom TP (mg/L)	0.583	0.088	0.246	85% reduction	58% reduction	< 0.050
		Mean bottom SRP (mg/L)	0.467	0.038	0.199	92% reduction	57% reduction	< 0.050
		Mean chlorophyll (ug/L)	47.63	25.17	19.08	47% reduction	60% reduction	< 15
		Mean Secchi transparency (ft)	4.27	6.28	5.41	46% increase	27% increase	12.1
	Early Fall peak (i.e. late August-early October)	Surface TP (mg/L)	0.130	0.081	0.115	38% reduction	11% reduction	NA
		Bottom TP (mg/L)	1.216	0.13	0.543	89% reduction	55% reduction	NA
		Bottom SRP (mg/L)	1.092	0.068	0.468	94% reduction	57% reduction	NA
		Chlorophyll (ug/L)	109.6	42.95	27.63	61% reduction	75% reduction	NA
		Secchi transparency (ft)	2.66	3.61	3.63	36% increase	37% increase	NA
Sediment		Net internal P loading (kg/summer)	3,723	1,150	1,062	69% reduction	71% reduction	< 400
		Net internal P loading (mg/m^2 d)	8.8	3.2	3.0	64% reduction	66% reduction	< 1.5
		Sediment diffusive P flux (mg/m^2 d)	15.01	9.53	10.66	37% reduction	29% reduction	< 1.5
		Redox-P (mg/g)	0.457	0.276	0.331	37% reduction	28% reduction	< 0.100
		Al-bound P (mg/g)	0.097	0.160	0.175	65% increase	80% increase	NA

influenced by the late September storm, resulting in lower transparency due to inorganic turbidity.

Cedar Lake P mass exhibited modest seasonal increases in 2018 (Fig. 14). However, post alum treatment late summer peaks in lake P mass were much lower in 2018 versus the pretreatment year 2010. Peak lake P mass was only 1,763 kg in 2018 compared to a maximum of > 4,000 kg in 2010. As indicated in James (2014, 2015), summer P mass increases were due almost entirely to internal P loading from anoxic sediment prior to alum treatment. Net internal P loading was substantial in 2010 at 3,723 kg (Table 3). In contrast, net internal P loading declined substantially to 1,150 kg and 1,062 kg in 2017 and 2018, respectively (Table 3). Thus, the 2018 net internal P loading rate represented a 71% reduction over the rate estimated for 2010. When normalized with respect to the time period used in the estimation of net internal P loading (kg/d), the rate

Table 3. Summer net internal phosphorus loading ($P_{net\ int\ load}$) estimates (bold font) for Cedar Lake in 2010 (pretreatment) and 2017-18 (post-treatment).

Summer	Period	$P_{tributary}$	$P_{discharge}$	$P_{retention}$	$P_{lake\ storage}$	$P_{net\ int\ load}$		
	(d)	(kg)	(kg)	(kg)	(kg)	(kg)	(kg/d)	(mg/m^2 d)
2010	97	445	238	207	3,931	**3,723**	**38**	**8.8**
2017	83	349	212	137	1,287	**1,150**	**14**	**3.2**
2018	87	279	122	157	1,227	**1,070**	**12**	**3.0**

was much lower in 2018 at 12 kg/d versus 2010, representing a 68% improvement over the 2010 rate of 38 kg/d (Table 3).

The pattern of seasonal P mass increase in the epilimnion versus the hypolimnion also changed in conjunction with the 2017 alum treatment (Fig. 15). For instance, the anoxic hypolimnion accounted for most of the of the seasonal P mass increase in 2010 (Fig. 15). By comparison, hypolimnetic P mass accumulation was minor in 2018, indicating continued suppression of net internal P loading (Fig. 15).

Changes in sediment chemistry and anaerobic diffusive phosphorus flux

Laboratory-derived anaerobic diffusive P fluxes declined substantially at many stations in July 2018 in conjunction with the 2017 alum treatment (Fig. 16). However, rates were still relatively high in 2018 and did not reflect the substantially decreased net internal P loading estimated via P mass balance from changes in lake water column P (Table 3). When all stations were considered, anaerobic diffusive P flux decreased by a mean 30% from 2017 (mean rate = 15.01 mg/m^2 d ± 0.85 SE) to 2018 (mean rate = 10.66 mg/m^2 d ± 0.66 SE, Fig. 17). Although the percent decline was important, the mean 2018 anaerobic diffusive P flux was still relatively high at 10.66 mg/m^2 d. This discrepancy suggested that laboratory-derived anaerobic diffusive P flux determinations were overestimating lake net internal P loading and should be viewed with caution. Typically, P fluxes determined from laboratory incubations are greater than those estimated from P mass balance (Nürnberg 2009).

Overall, mean (n = 27) redox-P remained lower in the upper 5 cm in 2018 compared to June 2017 (immediately before alum treatment), suggesting removal of sediment mobile P from recycling (Fig. 17). However, most of the reduction in redox-P occurred in 2017 after the alum treatment as there was approximately no further decline in the mean concentration in 2018. Although not statistically significant, the mean Al-bound P concentration increased slightly from 2017 to 2018 and was higher than pretreatment concentrations in June 2017 (Fig. 17). This pattern suggested that the Al floc layer was continuing to bind sediment P one year after treatment.

Vertically in the sediment column at station 2 concentrations of redox-P remained lower in the upper 5 cm sediment layer in 2018 relative to June 2017 (Fig. 18). Since redox-P is related to anaerobic diffusive P flux and, therefore, plays an important role in internal P loading (Nürnberg 1988, Pilgrim et al. 2007), lower redox-P concentrations in 2018 reflected continued internal P loading control in Cedar Lake. Aluminum-bound P concentrations remained elevated in the upper 5-cm layer in 2018, one year after the alum treatment, suggesting continued binding of P by the Al floc (Fig. 18).

Summary and recommendations

Mean summer (Jul-Oct) surface total P remained improved in 2018 and 22% lower than the 2010 pretreatment mean (Table 2). The 2018 mean was higher compared to 2017 in large part due to the watershed P loading event that occurred in September 2018. The mean summer chlorophyll concentration declined by 60% to only 19 µg/L in 2018 versus the pretreatment year 2010 (48 µg/L). The 2018 mean summer chlorophyll concentration was also lower compared to the 2017 mean of 25 µg/L, indicating continued algal biomass control one year after the alum treatment. The 2017 mean summer chlorophyll concentration was influenced by the occurrence of *Ceratium hirundinella*, a dinoflagellate (i.e., not cyanobacteria) that probably took advantage of severe alum treatment-induced P-limitation by assimilating sediment P before the treatment as a resting stage residing in the sediment. Mean summer Secchi transparency was deeper in 2018 compared to the pretreatment year 2010. However, the mean was lower by ~ 0.9 ft compared to the post-treatment summer of 2017.

Hypolimnetic post-alum treatment P remained low during the summer of 2018 until the end of July (Table 2). However, soluble P concentrations increased in the bottom waters in August, reaching a peak concentration of 0.467 mg/L. This pattern suggested that Al floc binding efficiency for P has diminished, allowing some of the internal P load to diffuse into the hypolimnion. Nevertheless, net internal P loading in 2018, determined by P mass balance, was reduced by ~ 70% relative to 2010. The 2018 post-treatment laboratory-derived mean diffusive P flux was also ~ 30% lower compared to the 2010 mean. However, this metric represented a

maximum potential rate and an overestimate compared to the substantial improvement in net internal P loading determined by mass balance. Mean sediment redox-P, which is the mobile P form that contributes to internal P loading, remained ~30% lower than the 2010 mean. In contrast, mean sediment Al-bound P was elevated relative to the pretreatment 2010 mean. Since Al-bound P directly quantified P binding specifically on the Al floc, trends suggested the Al floc has continued binding sediment P one year after treatment.

The next Al application is scheduled for late July 2019. The goal with lower dose alum treatments are to 1) spread costs for alum out over a longer time period and into smaller cost increments and 2) increase overall Al binding efficiency and binding capacity by exposing lower Al doses to sediment and hypolimnetic P. Monitoring and adaptive management approaches are being used to assess water quality and sediment response in order to adjust application timing and Al dosage if necessary to meet goals and expectations.

References

APHA (American Public Health Association). 2011. Standard Methods for the Examination of Water and Wastewater. 22th ed. American Public Health Association, American Water Works Association, Water Environment Federation.

Avnimelech Y, Ritvo G, Meijer LE, Kochba M. 2001. Water content, organic carbon and dry bulk density in flooded sediments. Aquacult Eng 25:25-33.

de Vicente I, Huang P, Andersen FØ, Jensen HS. 2008. Phosphate adsorption by fresh and aged aluminum hydroxide. Consequences for lake restoration. Environ Sci Technol 42:6650-6655.

Håkanson L, Jansson M. 2002. Principles of lake sedimentology. The Blackburn Press, Caldwell, NJ USA.

Hjieltjes AH, Lijklema L. 1980. Fractionation of inorganic phosphorus in calcareous sediments. J Environ Qual 8: 130-132.

James WF. 2012. Limnological and aquatic macrophyte biomass characteristics in Half Moon Lake, Eau Claire, Wisconsin, 2012: Interim letter report. University of Wisconsin – Stout, Sustainability Sciences Institute – Discovery Center, Menomonie, WI.

James WF. 2014. Phosphorus budget and management strategies for Cedar Lake, WI. University of Wisconsin – Stout, Sustainability Sciences Institute – Discovery Center, Menomonie, WI.

James WF. 2017. Phosphorus binding dynamics in the aluminum floc layer of Half Moon Lake, Wisconsin. Lake Reserv Manage 33:130-142.

James WF, PW Sorge, PJ Garrison. 2015. Managing internal phosphorus loading in a weakly stratified eutrophic lake. Lake Reserv Manage 31:292-305.

Mortimer CH. 1971. Chemical exchanges between sediments and water in the Great Lakes – Speculations on probable regulatory mechanisms. Limnol Oceanogr 16:387-404.

Nürnberg GK. 1988. Prediction of phosphorus release rates from total and reductant-soluble phosphorus in anoxic lake sediments. Can J Fish Aquat Sci 45:453-462.

Nürnberg GK. 2009. Assessing internal phosphorus load – Problems to be solved. Lake Reserv Manage 25:419-432.

Pilgrim KM, Huser BJ, Brezonik PL. 2007. A method for comparative evaluation of whole-lake and inflow alum treatment. Wat Res. 41:1215-1224.

Psenner R, Puckso R. 1988. Phosphorus fractionation: Advantages and limits of the method for the study of sediment P origins and interactions. Arch Hydrobiol Biel Erg Limnol 30:43-59.

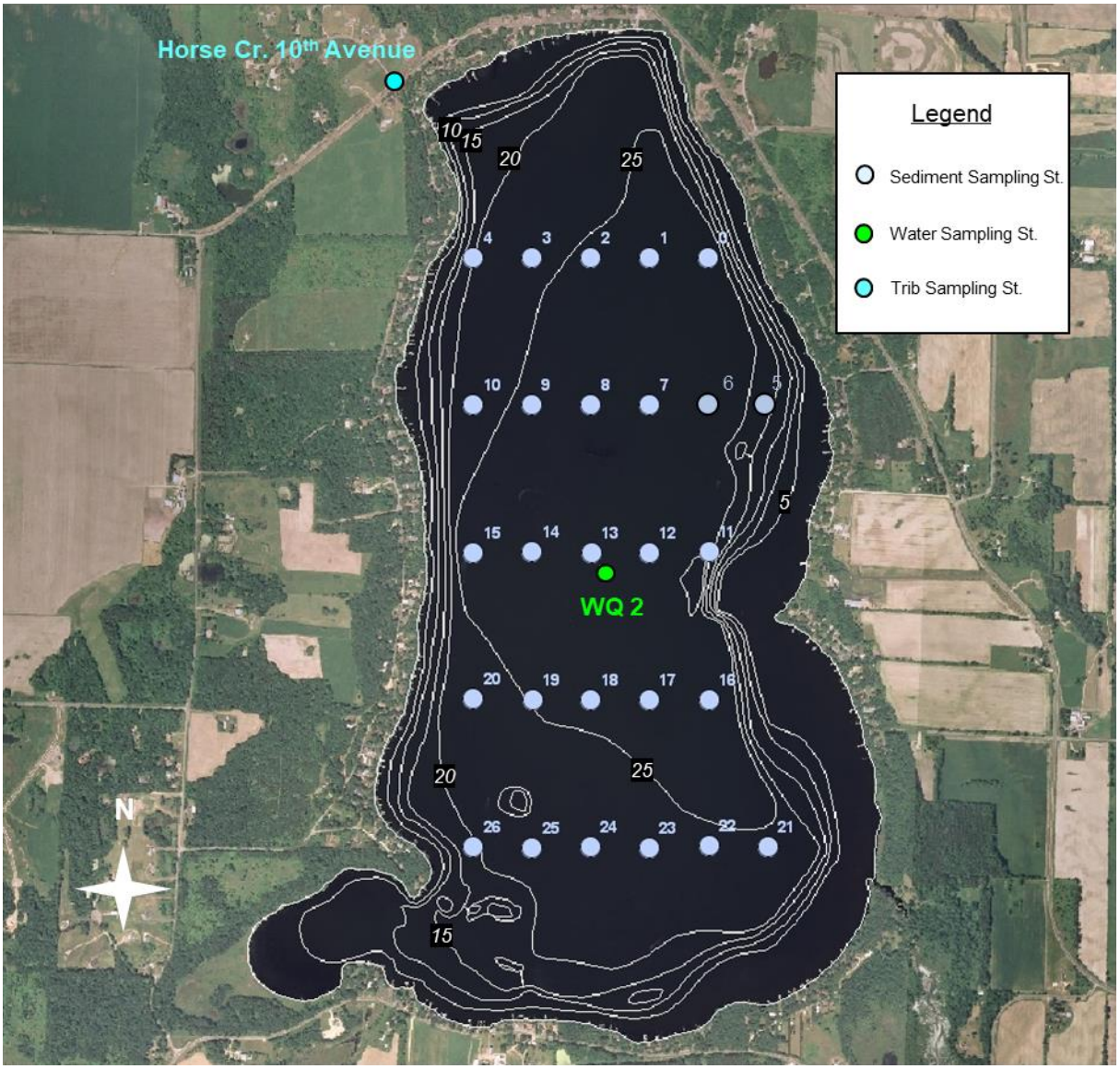

Figure 1. Sediment and water sampling stations.

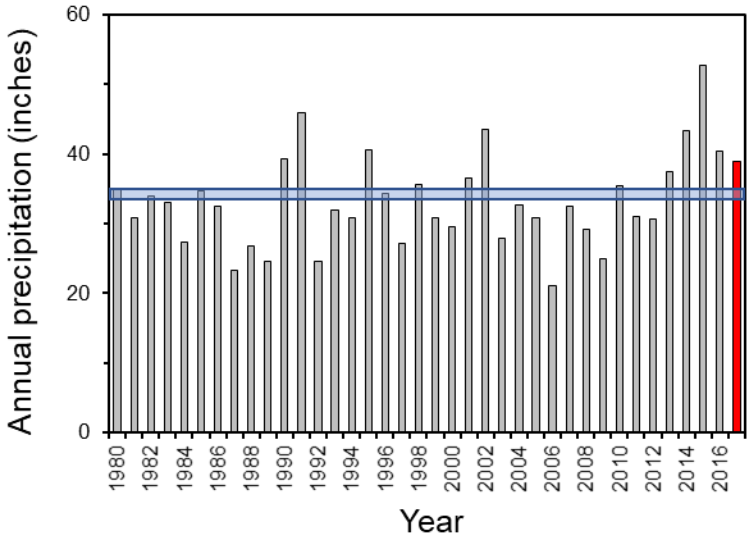

Figure 2. Variations in annual precipitation at Amery, WI. Blue horizontal line represents the average.

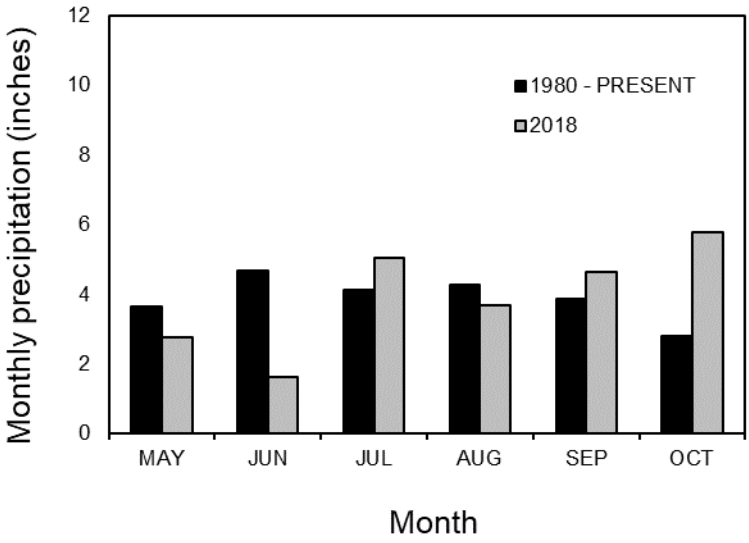

Figure 3. A comparison of average monthly precipitation.

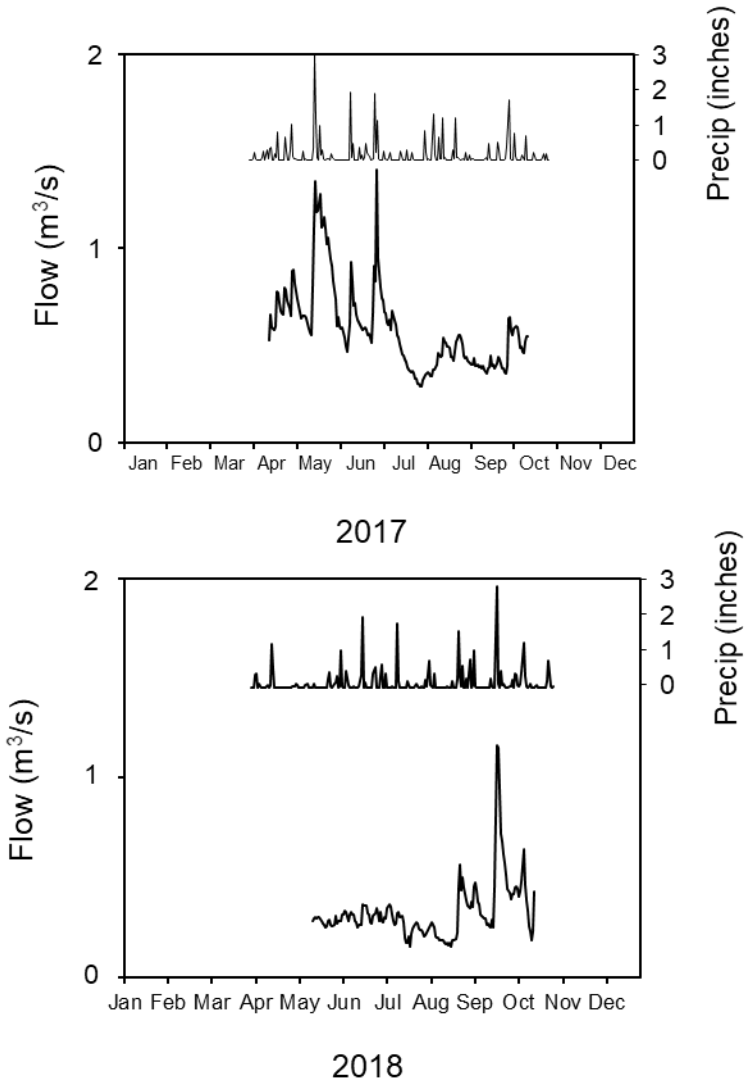

Figure 4. Seasonal variations in daily precipitation at Amery, WI, and flow for Horse Creek at 10th Ave.

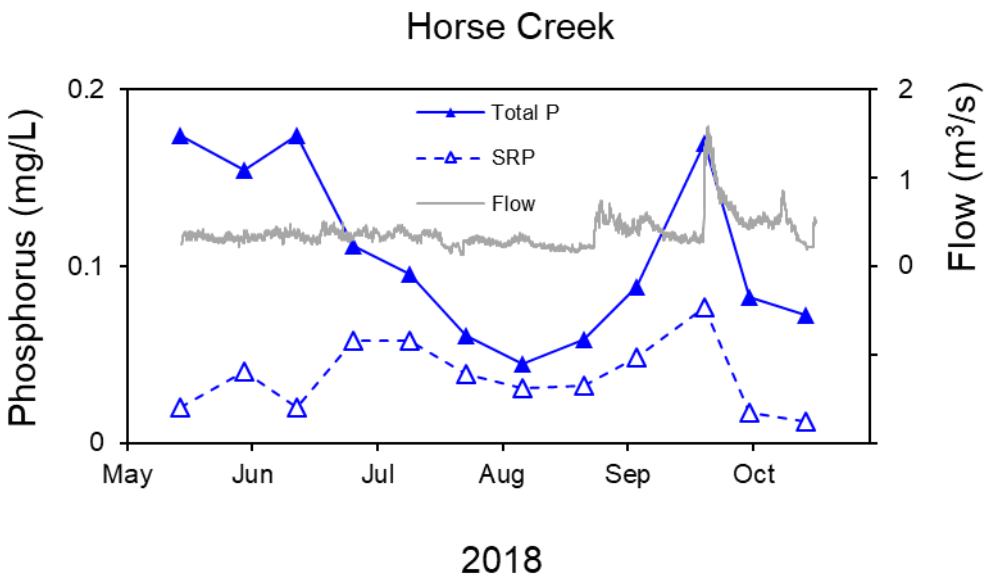

Figure 5. Seasonal variations in total phosphorus (P) and soluble reactive P (SRP) concentration at Horse Creek.

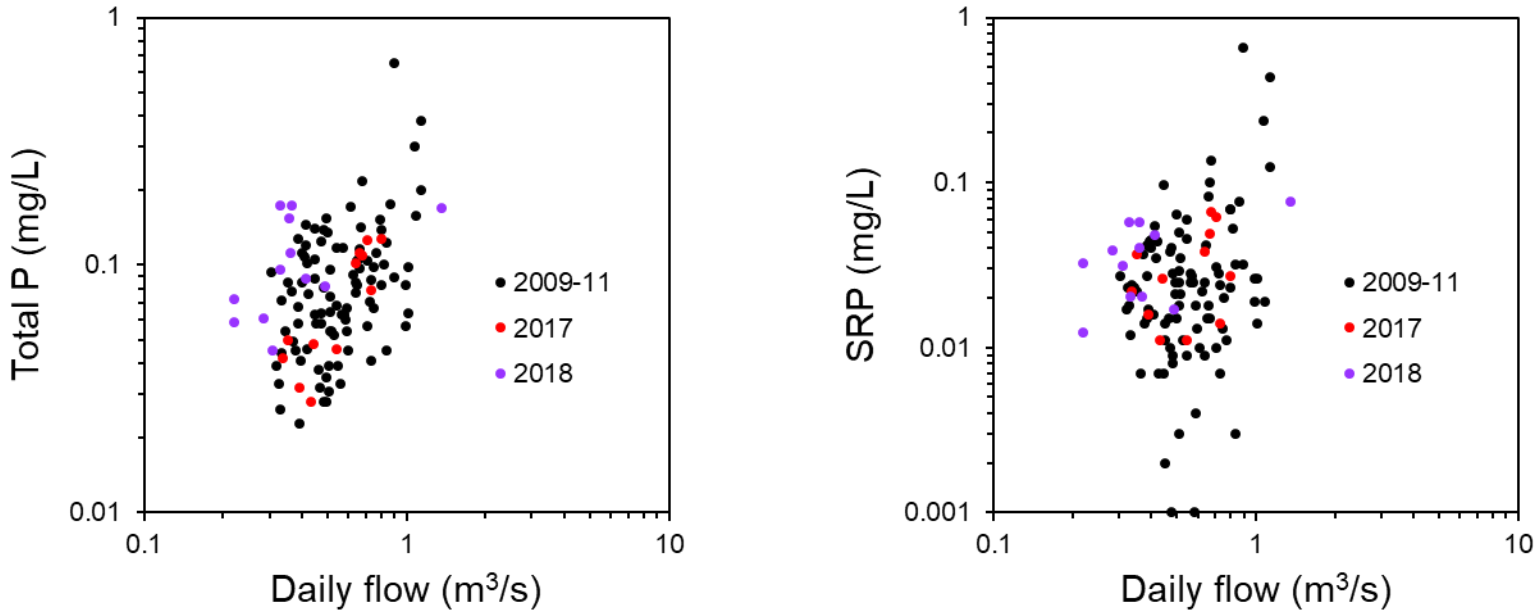

Figure 6. Phosphorus (P) concentration versus daily flow at Horse Creek.

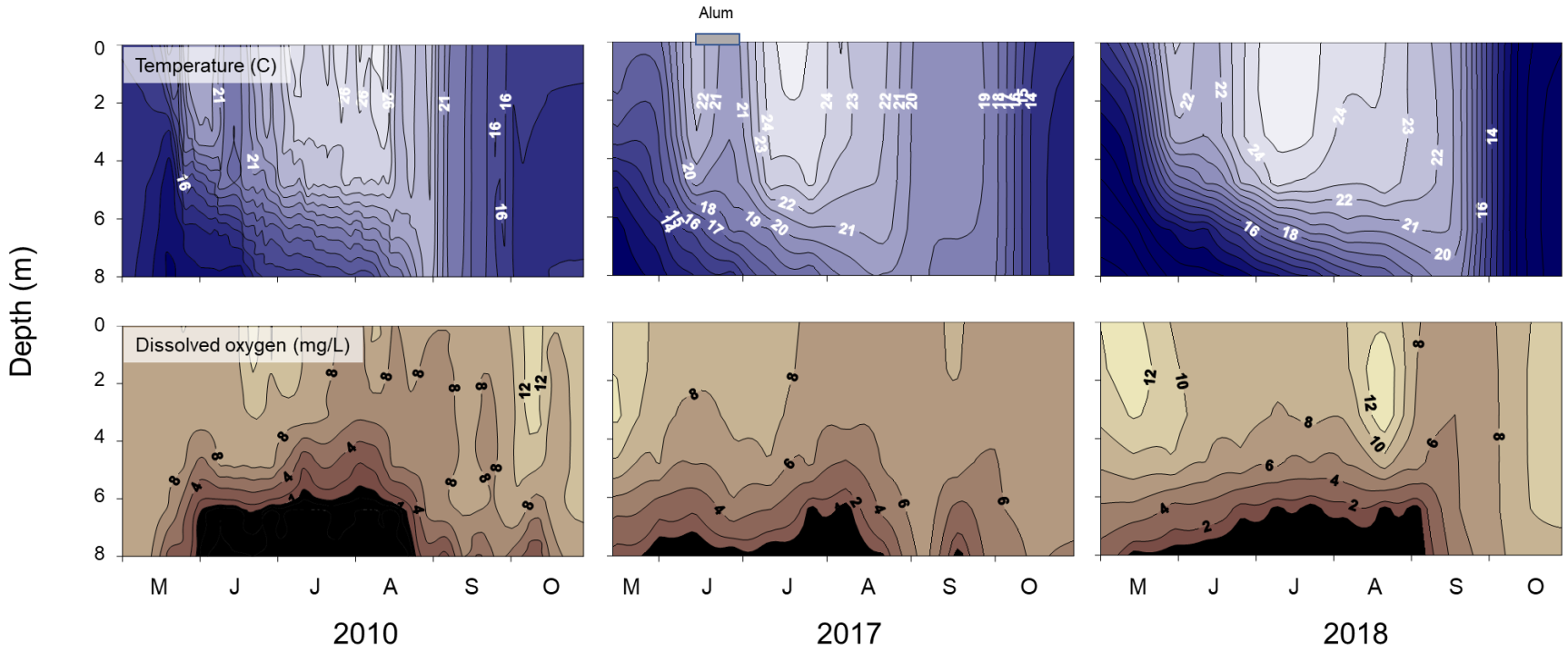

Figure 7. Seasonal and vertical variations in temperature (upper panel) and dissolved oxygen (lower panel) in 2010 (pre-treatment) and 2017-2018 (after alum treatment).

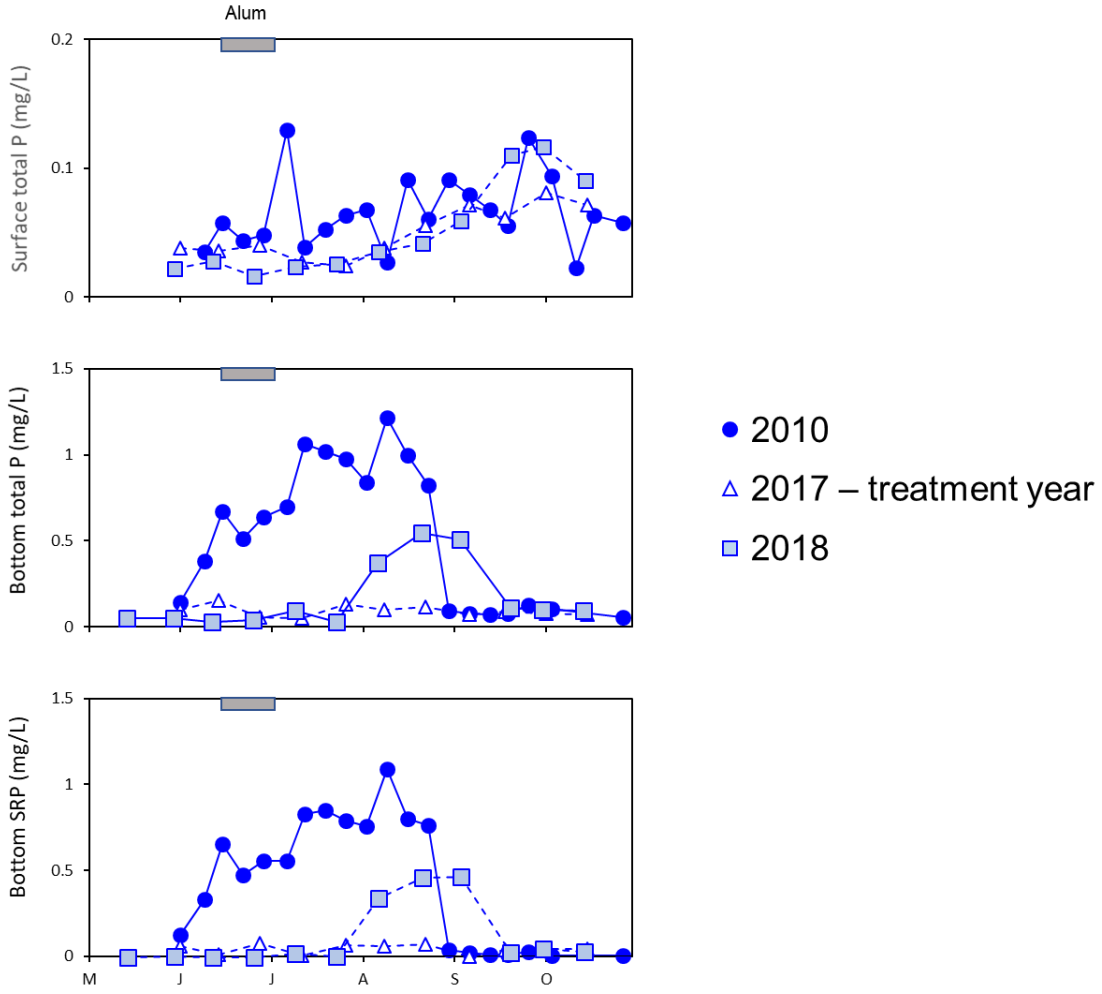

Figure 8. Seasonal variations in surface total phosphorus (P), bottom (i.e., ~ 0.25 m above the sediment-water interface) total P, and bottom soluble reactive P (SRP) during a pretreatment year (2010) and the post-alum treatment years 2017-18.

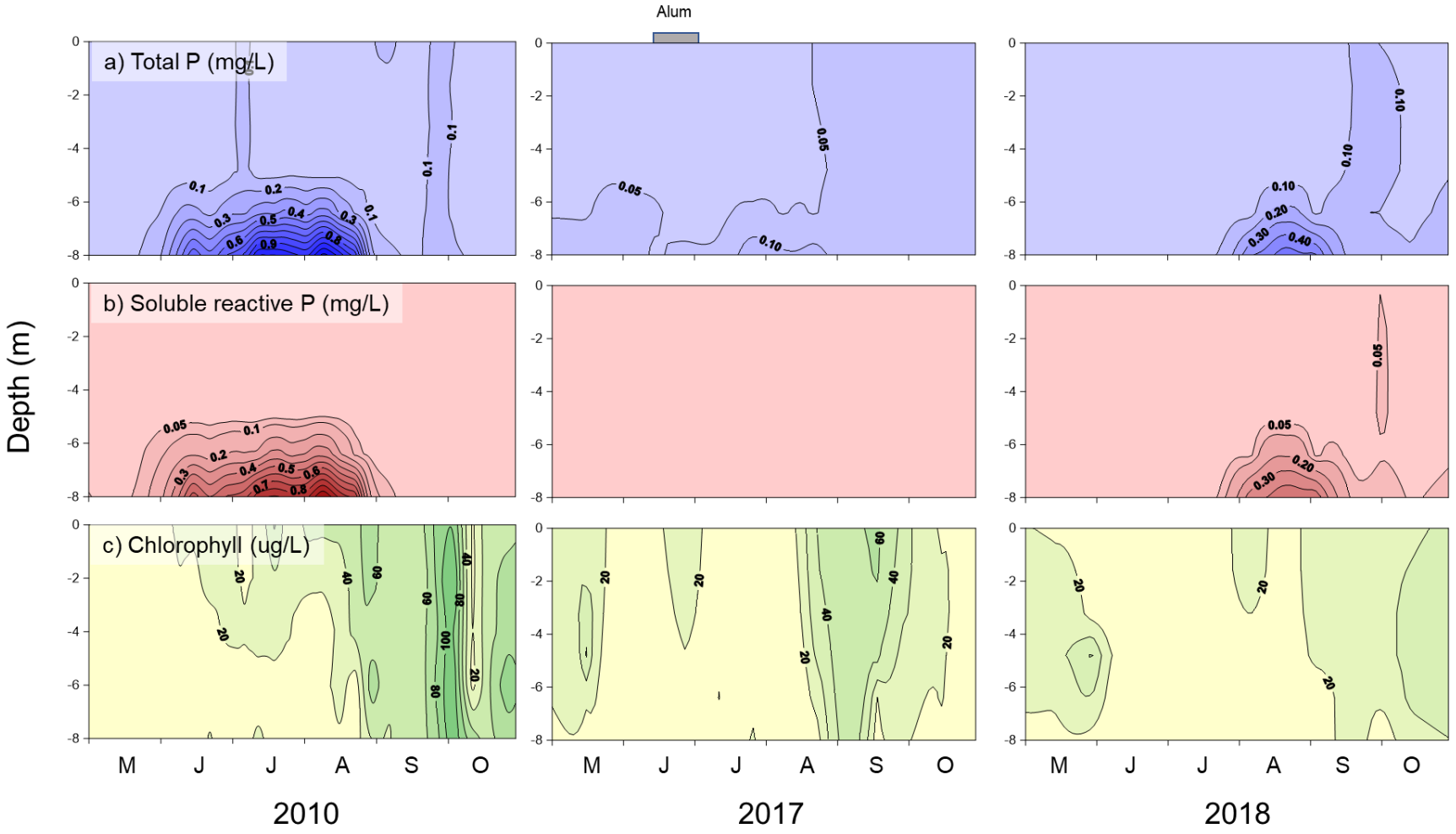

Figure 9. Seasonal and vertical variations in a) total phosphorus (P), b) soluble reactive P, and c) chlorophyll in 2010 (pretreatment) versus 2017-18 (post-treatment).

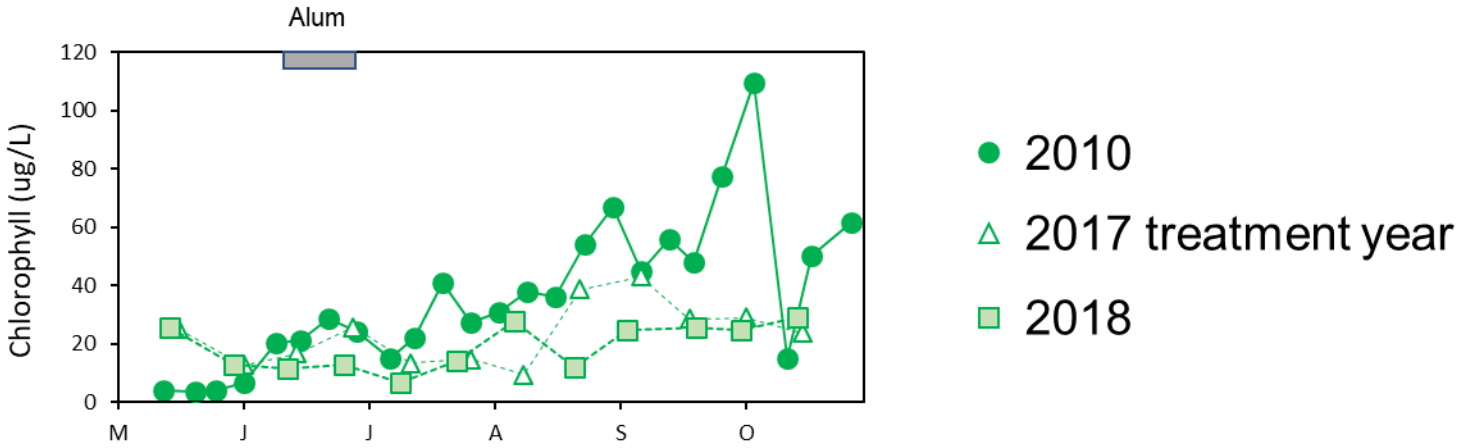

Figure 10. Seasonal variations in surface chlorophyll during a pretreatment year (2010) and the post-alum treatment years 2017-18.

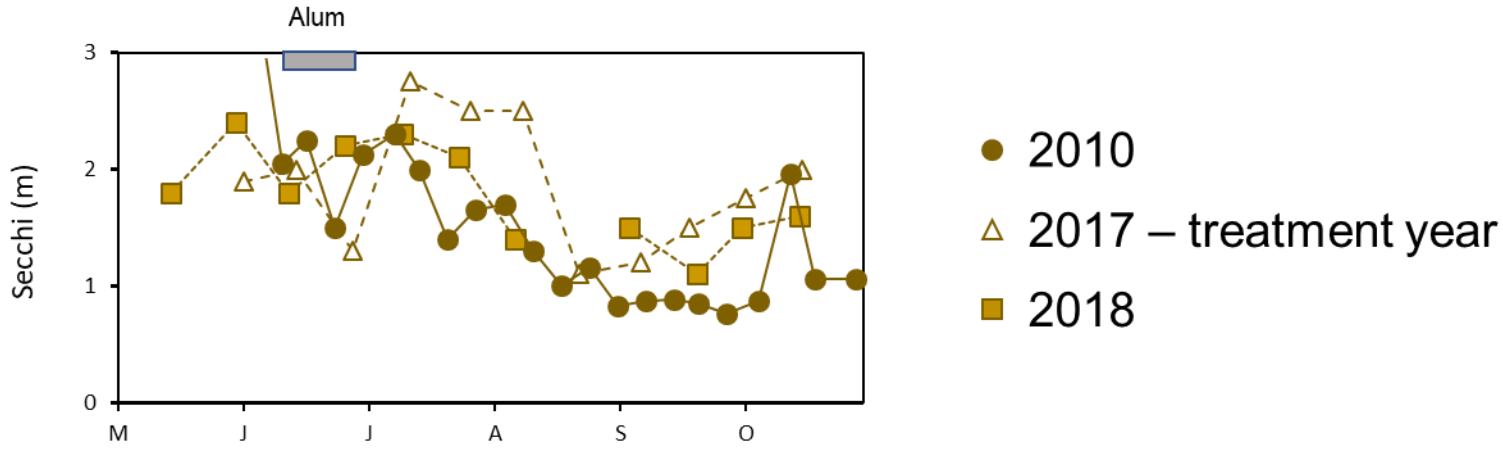

Figure 11. Seasonal variations in Secchi transparency during a pretreatment year (2010) and the post-alum treatment years 2017-18.

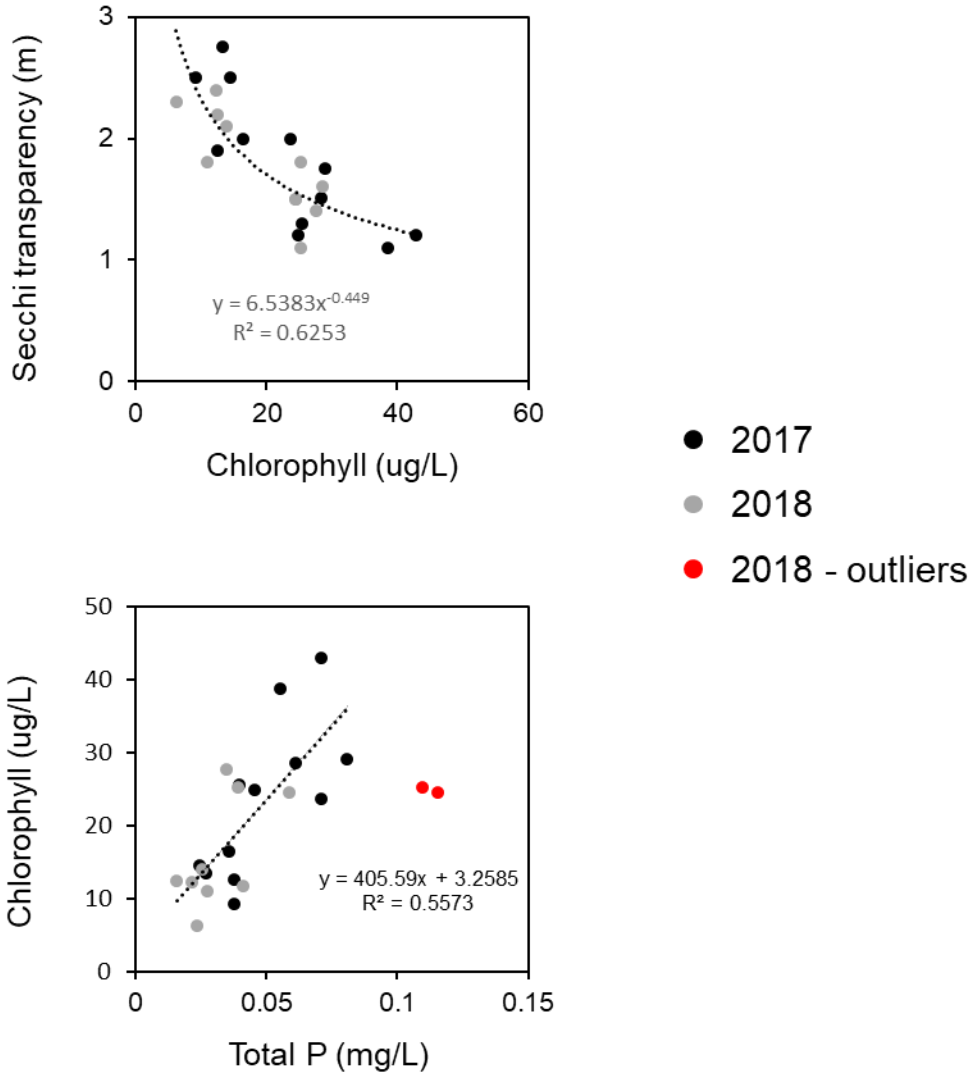

Figure 12. Relationships between Secchi transparency and chlorophyll (upper panel) and total phosphorus (P) versus chlorophyll (lower panel) during the summer 2017 and 2018.

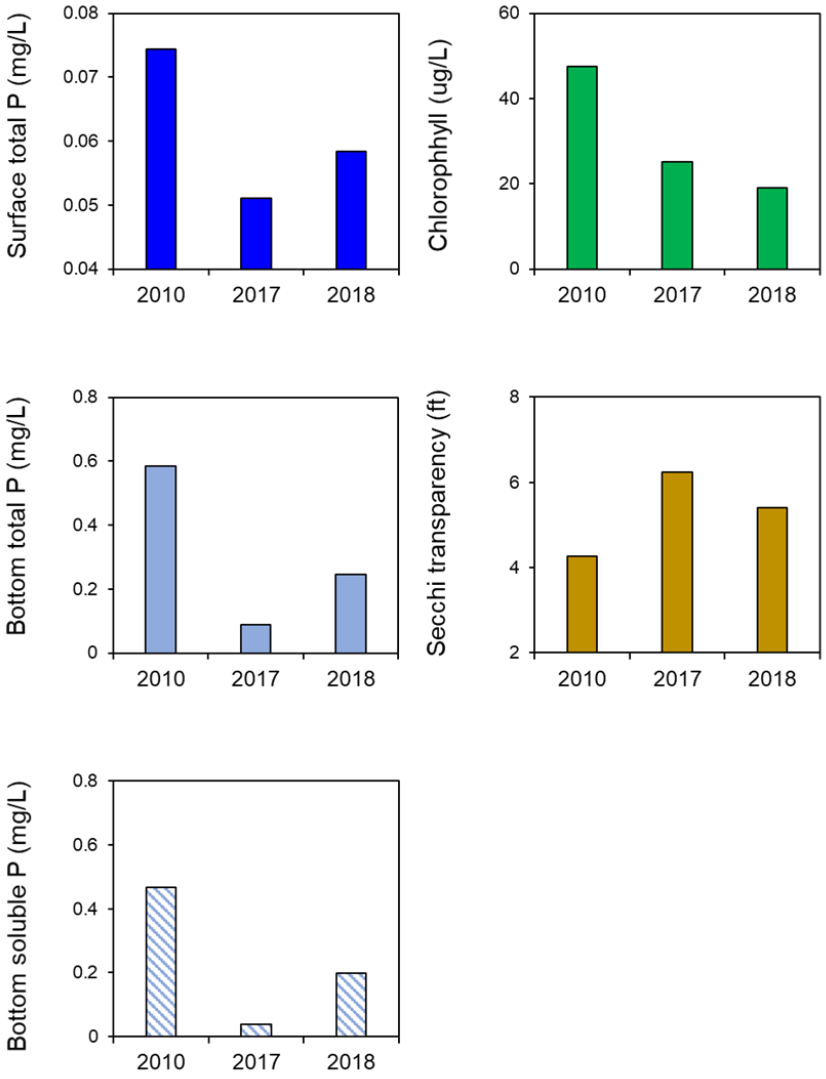

Figure 13. A comparison of mean summer (July-early October) summer concentrations of surface and bottom total phosphorus (P) and soluble reactive P (SRP), chlorophyll and Secchi transparency during a pretreatment year (2010) and the post-treatment years 2017-18.

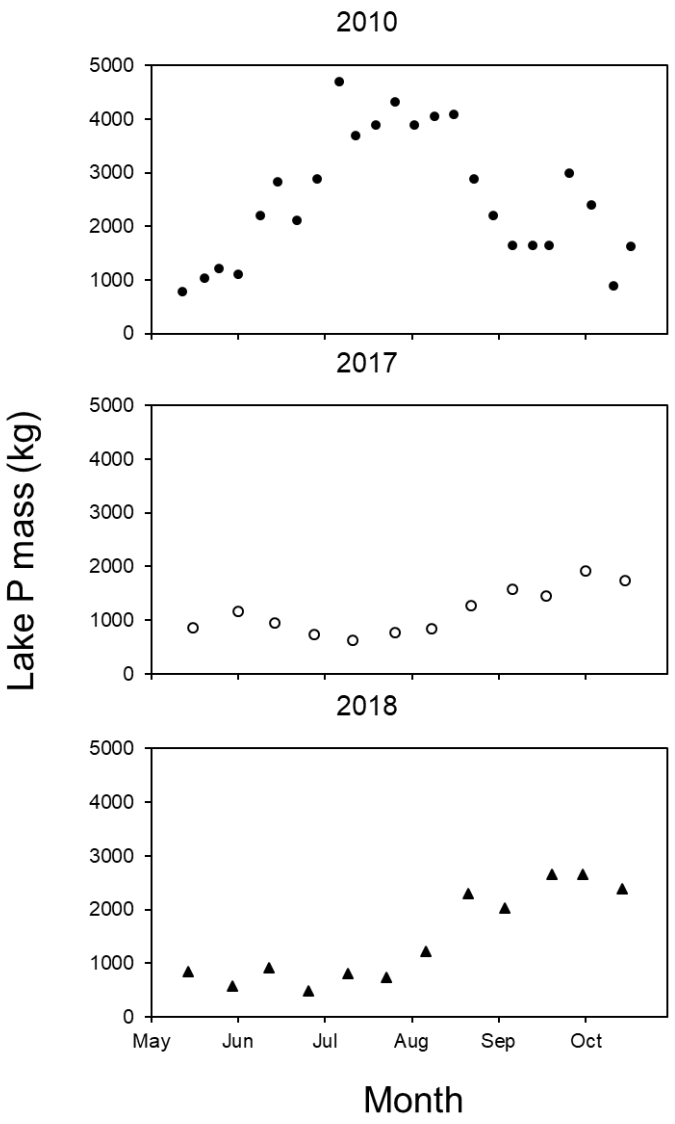

Figure 14. Seasonal variations in total phosphorus (P) mass during a pretreatment year (2010) and the post-treatment years 2017-18.

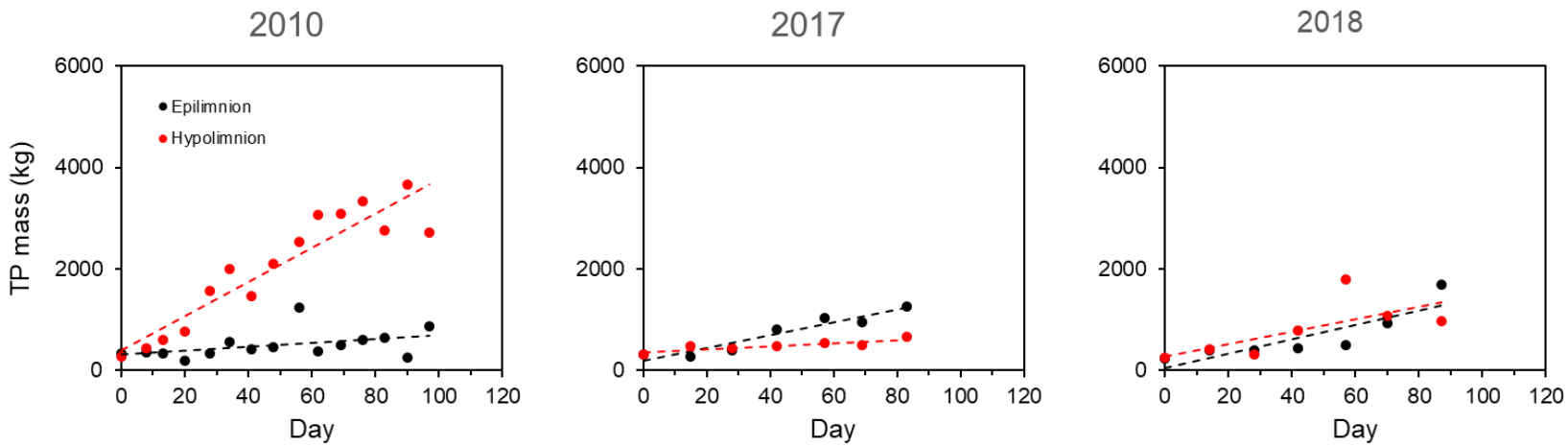

Figure 15. Seasonal variations in total phosphorus (P) mass in the epilimnion (i.e., 0-4 m) and hypolimnion (> 4 m) during a pretreatment year (2010) and the post-treatment years 2017-18.

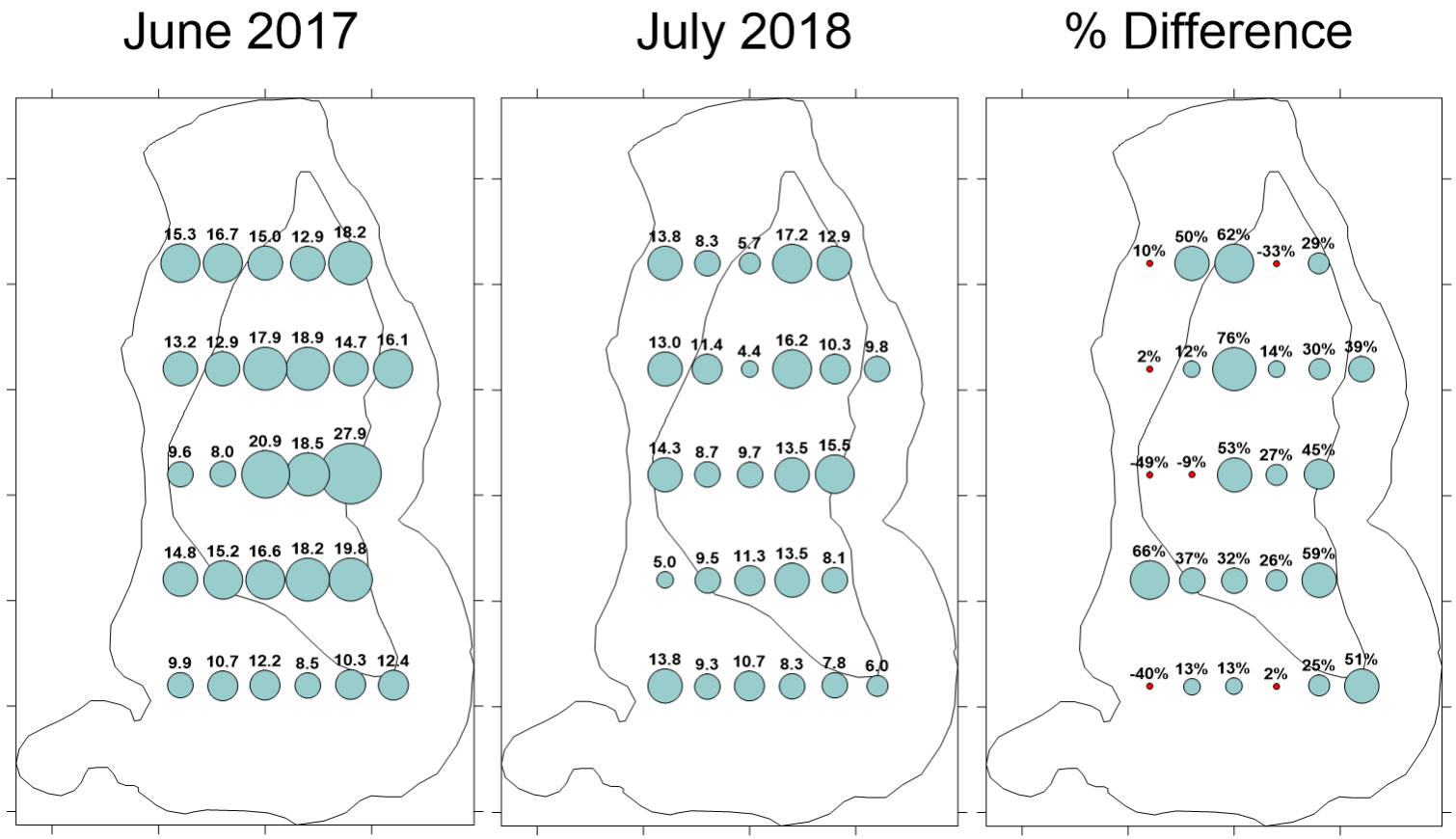

Figure 16. Spatial variations in anaerobic diffusive phosphorus (P) flux (mg/m^2 d) before (June 2017) and after (July 2018) alum application and the percent reduction or increase in the anaerobic diffusive P flux.

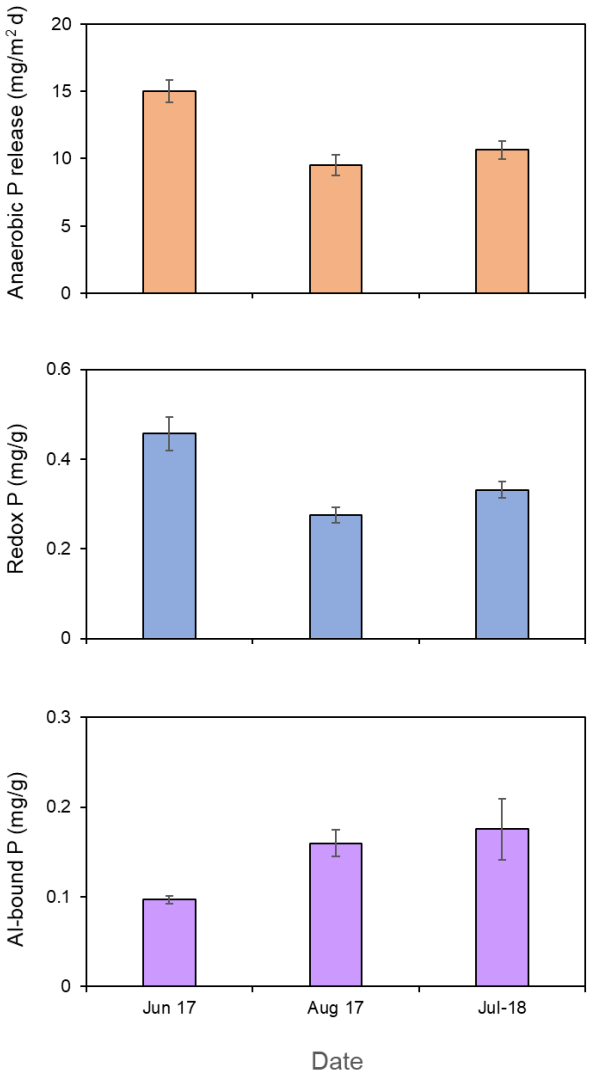

Figure 17. Changes in mean (n = 27, see Figure 1) rates of diffusive phosphorus (P) flux from sediment under anaerobic conditions mean sediment redox (i.e., the sum of the loosely-bound P and iron-bound P sediment fractions) P and aluminum (Al)-bound P concentrations adjusted for the upper 5-cm sediment layer for various years. June 2017 represents the pretreatment mean while August 2017 and July 2018 represent post-treatment means. Vertical lines represent ± 1 standard error.

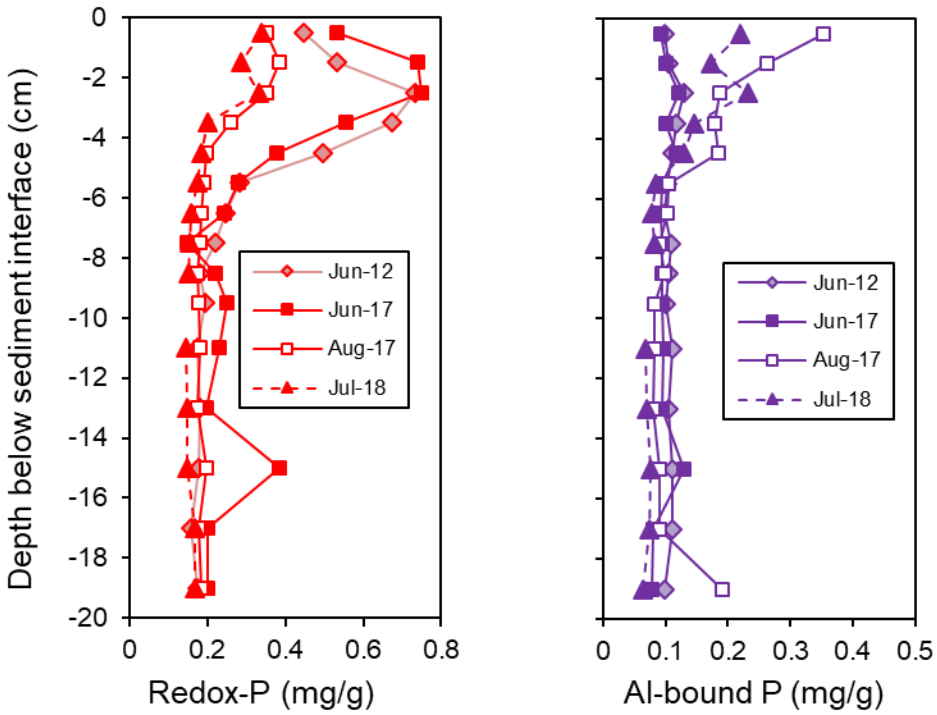

Figure 18. Vertical variations in sediment redox (i.e., the sum of the loosely-bound P and iron-bound P sediment fractions) phosphorus (P) and aluminum (Al)-bound P concentrations for a sediment core collected from station 2 (Figure 1) in June 2012, June 2017, August 2017, and July 2018. The sediment profile in June of 2012 and 2017 represent pre-treatment conditions while August 2017 and July 2018 represents post-alum treatment conditions.